

---

---

**STRUCTURAL MECHANICS AND STRENGTH  
OF FLIGHT VEHICLES**

---

---

## **Mathematical Modeling of Unloading a Linear Shock Cord Used in Aircraft Engineering**

**T. Z. Gimadieva and R. Sh. Gimadiev**

*Kazan State Power Engineering University, ul. Krasnosel'skaya 51, Kazan, 4200066 Tatarstan, Russia*

*e-mail: gimadievat@mail.ru*

Received April 15, 2013

**Abstract**—A mathematical model of accelerating a body along the inclined and horizontal rails under the tension force of the prestretched shock cord has been developed and numerically realized. The nonlinearity of load-strain dependence is taken into account. The shock cord is modeled as an absolutely flexible deformable thread. The results of numerical study are compared with the experiment data.

**DOI:** 10.3103/S1068799814010036

*Keywords:* mathematical model, shock cord, strain–tension curve, absolutely flexible thread.

At present, the systems, in which use is made of the energy of stretched rubber shock cords (e.g., for the dynamic regime of testing the aircraft equipment units [1] or in launchers for acceleration of unmanned aerial vehicles [2]), find their application in aircraft engineering. For this reason, of current interest now is the modeling of systems equipped with the rubber shock cords and proper account of their flexibility and elasticity. Large deformability of the materials being used as well as the wave processes in them [1] must be taken into account.

A variety of problems on the mathematical modeling of flexible linear elements with proper account for their strains can be successfully solved by using the thread motion equations [3].

In this paper, we present the mathematical model of moving a bogie along the inclined and horizontal rails under the action of tensile force in the pre-stretched shock absorber made from the rubber cord folded in several times. In making calculations, use is made of the static characteristic of shock absorber unloading that is obtained on the horizontal test bench (the Scientific-Research Institute of Aeroelastic Systems, Feodosiya). The data of numerical experiments are compared with those of field tests and we note their fair agreement.

### PROBLEM STATEMENT AND MATHEMATICAL MODEL

Figure 1 presents the layout of the test bench framework  $AB$  (in the general case, inclined and horizontal one at  $\alpha = 0$ ) and the bogie sliding along it. The bogie moves under the action of tensile force of the shock absorber  $OC$ , one end of which is fixed to the bogie and the other one is fixed at the point  $C$ . At the initial instant of time, the bogie is at the point  $B$  and the shock absorber is stretched ( $BC > l_a$ , where  $l_a$  is the shock absorber length in the unstrained state). When the bogie moves to the point  $A$ , the length of shock absorber is reduced ( $AC < BC$ ). In the process of bogie motion, it undergoes the gravity force  $G_g$ , standard pressure force  $N$ , friction force  $F_{fr}$ , drag  $Q$ , and force of the shock absorber tension  $T$ . Under unloading, the shock absorber is deformed due to displacement of its end  $O$  and (in the general case), due to the action of gravity forces. In this case, interaction between the shock absorber and the test bench surface is not taken into account. The shape of shock absorber is assumed to be rectilinear at the initial moment and in the particular case of motion.

The problem is to determine the bogie–shock absorber system motion.

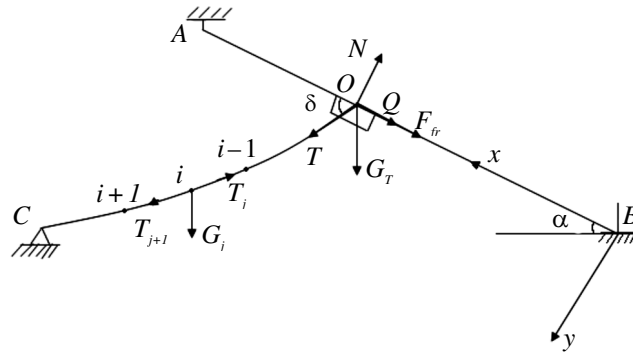


Fig. 1.

Let us assume that the shock absorber takes up only the stretching forces. We will simulate it as a stretchable ponderable ideally flexible thread.

Let us write the equations of the thread motion in the gravity force field in the projections onto the coordinate axes  $Bxy$  (Fig. 1):

$$\rho_a \frac{\partial v_x}{\partial t} = \frac{\partial}{\partial s} \left( \frac{T}{1 + \varepsilon} \frac{\partial x}{\partial s} \right) - \rho_a g \sin \alpha; \quad \rho_a \frac{\partial v_y}{\partial t} = \frac{\partial}{\partial s} \left( \frac{T}{1 + \varepsilon} \frac{\partial y}{\partial s} \right) + \rho_a g \cos \alpha, \quad (1)$$

where  $\rho_a$  is the linear density of the thread;  $g$  is the acceleration of gravity;  $\alpha$  is the angle of framework inclination to the horizon;  $v_x, v_y$  are the components of the thread motion velocity along the coordinate axes  $Bxy$ ;  $s$  is the Lagrange coordinate of the thread point counted from the point  $O$ ;  $T$  is the thread tension;  $\varepsilon$  is the relative thread elongation.

The equation of the bogie motion can be written in the following form:

$$m_b \frac{dV_b}{dt} = -F_{fr} + T \cos \delta - G_b \sin \alpha - c_b f_b \frac{\rho V_b^2}{2}, \quad (2)$$

where  $V_b$  is the bogie velocity;  $\delta$  is the angle between the tangent to the thread at the point  $O$  and the framework (Fig. 1);  $c_b$  is the coefficient of the bogie resistance force;  $f_b$  is the characteristic area of the bogie, and  $\rho$  is the air density.

At bogie sliding along the framework, the friction force will be

$$F_{fr} = \mu N, \quad (3)$$

where  $\mu$  is the coefficient of sliding friction.

Taking into account that the bogie moves only towards the  $Bx$  axis, we shall find

$$N = G_b \cos \alpha + T \sin \delta. \quad (4)$$

The differential equations of motion (1), (2) are supplemented with the following kinematical relations for the thread:

$$\frac{\partial x}{\partial t} = v_x, \quad \frac{\partial y}{\partial t} = v_y; \quad (5)$$

kinematical relation for the bogie:

$$\frac{dx_b}{dt} = V_b; \quad (6)$$

as well as the geometric and physical relations for the thread:

$$\left( \frac{\partial x}{\partial s} \right)^2 + \left( \frac{\partial y}{\partial s} \right)^2 = (1 + \varepsilon)^2, \quad (7)$$

$$T = T(\varepsilon). \quad (8)$$

Initial conditions can be represented in the form:

$$y(0,s) = \frac{y_c}{l_a} s; \quad x(0,s) = \frac{x_c}{l_a} s; \quad v_x(0,s) = 0, \quad v_y(0,s) = 0, \quad x_T(0) = 0, \quad V_T(0) = 0. \quad (9)$$

Boundary conditions can be represented as:

$$x(t,0) = x_T; \quad y(t,0) = 0; \quad x(t,l_a) = x_c; \quad y(t,l_a) = y_c, \quad (10)$$

where  $x_c, y_c$  are the point C coordinates (Fig. 1).

Then, we will impose the following additional restriction:

$$T(t, s) \geq 0.$$

In order to solve the system of equations (1), (2), (5), and (6), we will use the finite-difference method. Let us introduce into consideration the discrete domain  $s_i = i\Delta s$ ,  $t_j = j\Delta t$  ( $i = 1, \dots, n$ ;  $j = 1, 2, \dots$ ;  $\Delta s = l_a/n$  is the length of unstrained element).

By using the central differences to approximate the derivatives, we can write the system of equations (1), (2), (5), (6) in the finite difference form according to the explicit scheme:

$$\begin{aligned} V_{x,i}^{j+1/2} &= V_{x,i}^{j-1/2} + \frac{\Delta t}{\rho_a \Delta s} \left( T_{i+1}^j \cos \delta_{i+1}^j - T_i^j \cos \delta_i^j - \rho_a g \Delta s \sin \alpha \right); \\ V_{y,i}^{j+1/2} &= V_{y,i}^{j-1/2} + \frac{\Delta t}{\rho_a \Delta s} \left( T_{i+1}^j \sin \delta_{i+1}^j - T_i^j \sin \delta_i^j + \rho_a g \Delta s \cos \alpha \right); \\ V_b^{j+1/2} &= V_b^{j-1/2} + \frac{\Delta t}{m_b} \left( -F_{fr}^j + T_1^j \cos \delta_1^j - G_b \sin \alpha - c_b f_b \frac{\rho (V_b^{j-1/2})^2}{2} \right), \end{aligned} \quad (11)$$

$$x_i^{j+1} = x_i^j + \Delta t \cdot V_{x,i}^{j+1/2}; \quad y_i^{j+1} = y_i^j + \Delta t \cdot V_{y,i}^{j+1/2}; \quad x_b^{j+1} = x_b^j + V_b^{j+1/2} \Delta t.$$

The length of the strained  $i$ th element will then be:

$$l_1^j = \sqrt{(x_T^j - x_1^j)^2 + (y_T^j - y_1^j)^2}, \quad i=1; \quad l_i^j = \sqrt{(x_i^j - x_{i-1}^j)^2 + (y_i^j - y_{i-1}^j)^2}, \quad i=2, \dots, n; \quad (12)$$

$$\cos \delta_1^j = \frac{x_1^j - x_T^j}{l_1^j}, \quad \sin \delta_1^j = \frac{y_1^j - y_T^j}{l_1^j}, \quad i=1; \quad \cos \delta_i^j = \frac{x_i^j - x_{i-1}^j}{l_i^j}, \quad \sin \delta_i^j = \frac{y_i^j - y_{i-1}^j}{l_i^j}, \quad i=2, \dots, n. \quad (13)$$

The relative elongation can be expressed as:

$$\varepsilon_i^j = \begin{cases} l_i^j / \Delta s, & \text{if } l_i^j / \Delta s \geq 1, \\ 0 & \text{if } l_i^j / \Delta s < 1. \end{cases} \quad (14)$$

The tension is presented as

$$T_i^j = T(\varepsilon_i^j). \quad (15)$$

The coordinates of points  $i$  at the initial instant of time will be the following:

$$x_i = \frac{x_c}{n} i; \quad y_i = \frac{y_c}{n} i \quad (i = 1, \dots, n-1). \quad (16)$$

Since the differential scheme being used is explicit, in the numerical solution there may appear the high-frequency oscillations in magnitude values. In order to suppress these oscillations, use is made of the direct correction of velocities for nodal points of computational grid [4] by the formulas:

$$\tilde{V}_x = V_x + \beta \frac{\partial^2 V_x}{\partial s^2}; \quad \tilde{V}_y = V_y + \beta \frac{\partial^2 V_y}{\partial s^2}. \quad (17)$$

The program for modeling the bogie motion along the test bench framework under the action of tensile force of rubber shock absorber was formulated in accordance with the mathematical model presented.

TEST PROGRAM DEVELOPMENT

The program was verified by test calculations.

The value of maximal slackness in the thread stretched between two fixed supports (distance between them is equal to  $a$ ) under the action of gravity force is compared with the analytical solution [5] by the following formula:

$$y_{\max} = \frac{a^2(1+\varepsilon)}{8E\varepsilon} \rho_a g, \tag{18}$$

where

$$\varepsilon = \sqrt[3]{\frac{\gamma}{2} + \left[ \left( \frac{\gamma}{2} \right)^2 - \left( \frac{\gamma}{3} \right)^3 \right]^{\frac{1}{2}}} + \sqrt[3]{\frac{\gamma}{2} - \left[ \left( \frac{\gamma}{2} \right)^2 - \left( \frac{\gamma}{3} \right)^3 \right]^{\frac{1}{2}}};$$

$\gamma$  is the loading parameter that can be determined by the formula

$$\gamma = (\rho_a g)^2 a^2 / (24E^2).$$

Numerical calculations are correlated with the analytical solution.

The shock absorber oscillation frequency is compared with the string oscillation frequency in the eigentone [6]:

$$v = \frac{1}{2} \sqrt{\frac{T}{ml}}, \tag{19}$$

where  $m$  is the mass of string.

The initial disturbance was assigned in accordance with the node velocity in the string middle  $V_i = 20$  m/s ( $i = n/2, n = 50$ ) towards its normal. The data of numerical calculations differ from those obtained by formula (19) by no more than 2 %.

Based on test calculations, the coefficient  $\beta$  was taken to be  $0.015 \Delta s^2$ . The integration step  $\Delta t$  was chosen by calculations using the condensed grids in the stability region according to the Courant criterion  $\Delta t < \Delta s \sqrt{\rho_a / E_a}$ , where  $E_a$  is the ultimate modulus of elasticity of the shock absorber.

In the course of program development, we also modeled:

- propagation of longitudinal wave in the shock absorber according to the linear and nonlinear laws  $T(\varepsilon)$ ;
- reflection of longitudinal wave from the fixation point;
- standing waves;
- resonance.

COMPARISON OF NUMERICAL AND FULL-SCALE EXPERIMENTS ON THE HORIZONTAL TEST BENCH

Numerical and full-scale experiments were compared in order to verify correspondence between the model developed and the real process and estimate the confidence of the velocity values being computed.

Figure 2 presents the mean static diagram of unloading for a new rubber shock absorber of  $\varnothing 20$  mm that is folded in 20 times. The graph was constructed by the results obtained in five experiments on the test bench in the Scientific-Research Institute of Aeroelastic Systems, Feodosiya.

The experimental points were approximated by the least-squares method using the polynomial:

$$T(\varepsilon) = 598.01\varepsilon^5 - 1461.3\varepsilon^4 + 1376.8\varepsilon^3 - 596.66\varepsilon^2 + 126.63\varepsilon + 2.6475.$$

Using the same shock absorber of 50 m in length and different initial elongation, a number of experiments was conducted to accelerate a bogie with a mass of 47 kg on the horizontal test bench.

Figure 3 presents the velocity-time diagrams obtained for two experiments with the initial conditions being equal. The maximal velocities obtained in both full-scale experiments differ by 8 %; the reason for this that it is impossible to provide the stable experiment conditions on the test bench. When the rubber shock absorbers are used in the full-scale experiments, it is possible to obtain the velocities of up to 65 m/s.

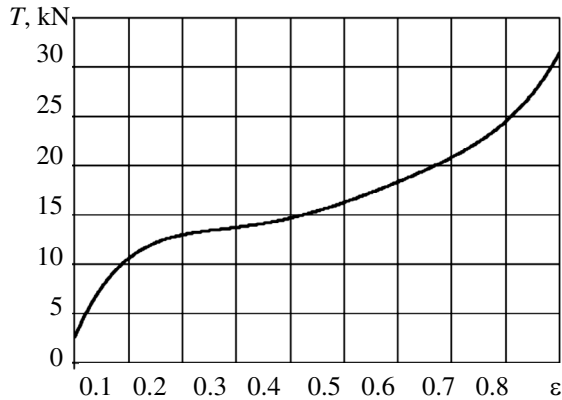


Fig. 2.

Fig. 2. Diagram of unloading for a new rubber shock absorber folded in 20 times.

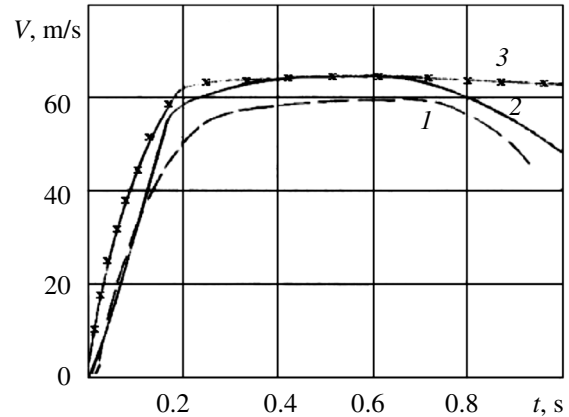


Fig. 3.

Fig. 3. Variation of the bogie velocity in motion at initial elongation of the shock absorber  $\varepsilon_a = 0.9$ : 1, 2—experiment; 3—calculation.

Figure 3 presents also the estimated velocity-time dependence for the bogie moving under the action of the shock absorber tension force. As can be seen from this figure, the bogie velocity obtained experimentally increases slower than the calculated one. The maximal velocity in calculations is larger than the experimentally obtained one by 0 – 8 %. This difference is because the friction in the shock absorber motion along the test bench surface is not taken into account.

#### USE OF RUBBER SHOCK ABSORBERS FOR ACCELERATING A BOGIE ON THE INCLINED TEST BENCH

In order to examine a possibility of using the inclined test bench with the adjusted angle of the framework slope and impart thereby the initial flight velocities for small-size products, we conducted the numerical experiments of the bogie motion along the inclined framework at the angles of its installation  $\alpha = 10^\circ$  and  $30^\circ$  and different bogie masses  $m_b = 25, 50,$  and  $100$  kg. The length of this inclined framework is  $L = 45$  m.

The calculations were conducted when the number of shock cord folds was  $k = 4, 10, 18$ . Tension of the shock cord was assumed to be proportional to the number of folds.

The point  $C$  coordinate was determined from the condition that at the initial time instant (when the bogie is at the point  $B$ ) the shock absorber is stretched by 80 %, i.e.,  $BC = 1.8l_a$ . The distance from the point  $A$  up to the point  $C$  (Fig. 1) was assumed to be equal to the length of shock absorber in its unstrained state:  $AC = l_a$ .

The friction coefficient was taken  $\mu = 0.1$  at the bogie motion along the framework. The coefficient of the bogie resistance was  $c_b = 0.95$ , and the specific area was  $f_b = 0.25$  m<sup>2</sup>.

Figure 4 presents the estimated dependences of the bogie velocity on its displacement  $V_b(v_b)$ . Curves 1, 2, and 4 illustrate how the number of shock cord folds influence on the bogie velocity variation. Curves 4,

5, and 6 show the influence of the bogie mass on its motion. Solid curves are drawn up by calculations at  $\alpha = 10^\circ$  and the dashed-line curve — at  $\alpha = 30^\circ$ .

Figure 5 presents the graphs of varying the tensile force along the length of the shock absorber (the dimensionless Lagrange coordinate of shock absorber is plotted as the abscissas) for different instants of time with their corresponding displacements of the bogie with a mass of 25 kg and the framework slope  $\alpha = 30^\circ$  and the number of the shock cord folds  $k = 10$ . As is seen from these graphs, the shock absorber tension decreases first in the region of the bogie fixation; this disturbance propagates further towards to the fixed point and tension in the vicinity of the point C drops to zero, when the bogie reaches the framework end.

As is seen from the graphs (Fig. 5), the tension at the point of shock absorber fixation to the bogie on the section of the bogie motion from 4 to 45 m changes insignificantly. Nonetheless, we see from the graph of velocity variation (Fig. 4, dashed-line curve) that acceleration on this section changes significantly, and starting from a value of  $x_b = 30$  m, the bogie velocity decreases. This is because the projection of the shock absorber tensile force onto the direction of the bogie motion decreases: at  $x_b = 24$  m  $\delta = 77^\circ$  and  $\cos \delta = 0.223$ ; at  $x_b = 45$  m  $\delta = 79^\circ$ , and  $\cos \delta = 0.188$ .

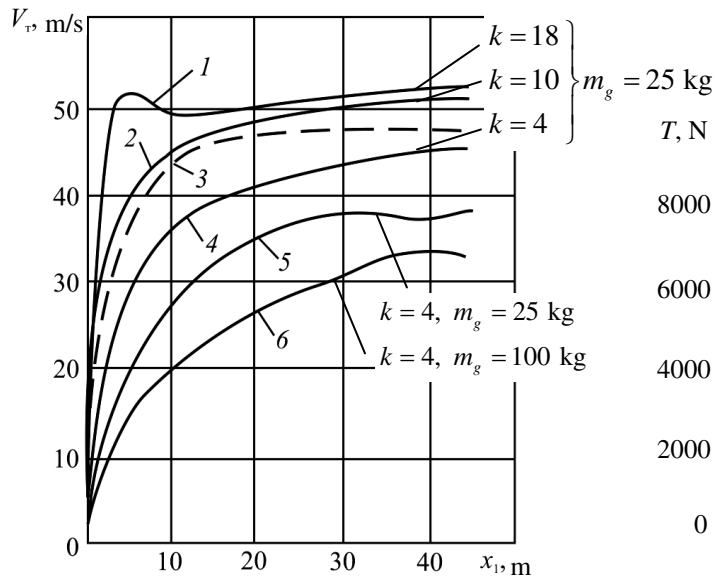


Fig. 4.

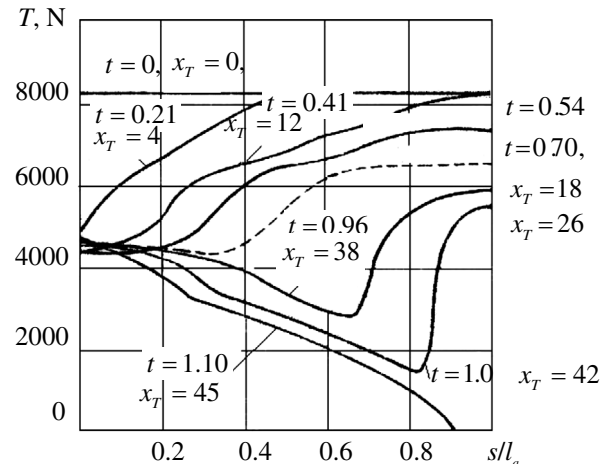


Fig. 5.

Fig. 4. Dependence of bogie velocity on displacement: —  $\alpha = 10^\circ$  ---  $\alpha = 30^\circ$ .

Fig. 5. Variation of tensile force in the shock absorber in time  $m_b = 25$  kg,  $k = 10$ ,  $\alpha = 30^\circ$ .

Figure 6 presents the shock absorber shape for displacements of the bogie along the test bench framework at  $x_b = 0$  m,  $x_b = 24$  m, and  $x_b = 45$  m. In this case, the influence of the shock absorber shape on the bogie motion manifests itself most clearly.

The maximal velocity, which the bogie can reach as the number of shock cord folds increases, is restricted by that the rate of the shock absorber unloading is finite, and this fact is the most evident in Fig. 4. When the number of the shock absorber folds is increased up to 18, the bogie velocity with a mass of  $m_b = 25$  kg increases (at the section, where the displacements are  $x_b < 6$  m) by 70 and 22 % as compared with the number of the shock cord folds  $k = 4$  and  $k = 10$ . Due to the presence of large accelerations in the initial section of the bogie motion, the tension in the shock absorber fails to redistribute along its entire

length; at the time instant, when the bogie displaces by 6 m, the tension on the section of the shock absorber to the bogie drops to zero and it moves with the negative acceleration up to  $x_b = 14$  m and tension in the region of the shock absorber fixation amounts to 702 N. Further, the bogie velocity increases insignificantly.



Fig. 6. Shape of the shock absorber in motion: (a)  $m_b = 25$  kg;  $k = 10$ ;  $\alpha = 30^\circ$ ; (b)  $m_b = 25$  kg;  $k = 10$ ;  $\alpha = 10^\circ$ .

Figure 6 presents the shock absorber shape for  $m_b = 25$  kg;  $k = 10$ ;  $\alpha = 10^\circ$ . By comparing Figs. 6a and 6b, it should be noted that nonuniformity of tension distribution along the shock absorber length and curvature at the motion end at  $\alpha = 10^\circ$  are larger than those at  $\alpha = 30^\circ$  (since at  $\alpha = 10^\circ$ , the bogie accelerates much more rapidly than at  $\alpha = 30^\circ$ ).

Use of a shock cord of  $\varnothing 20$  mm folded in 4–18 times will make it possible to accelerate the bogie with a mass of 25–100 kg with the framework slope 10–30° up to velocities 23–53 m/s (for comparison, according to the reference data [7], the sound velocity in rubber is equal to 54 m/s.).

## CONCLUSIONS

In order to simulate the unloading of the rubber shock cords, it seems to be rational to use the equation of thread motion and assign the physical relation in the form of nonlinear law (Fig. 2).

The mathematical model and numerical algorithm for tests on the horizontal and inclined test benches were developed with proper regard for nonlinearity of the rubber shock absorber unloading. The numerical experiments according to the algorithm developed agree quite well with the full-scale tests.

Using the rubber shock absorber, a velocity of up to 64 m/s can be attained on the horizontal stand, while on the inclined stand—a velocity of up to 53 m/s.

## REFERENCES

1. Gimadieva, T.Z., Comparison of Two Methods for Calculating the Tension Force in the Linear Shock Absorber, *IX Dal'nevostochnaya konferentsiya po myagkim obolochkam* (IXth Far Eastern Conference on Soft Shells), Vladivostok, pp. 78–80, 1991.
2. Alenchenkov, G.S., Launching Devices. Simulation of Unmanned Aerial Vehicles Launching, *Sovrenennoe Mashinostroenie. Nauka i Obrazovanie*, 2011, no. 1, pp. 108–115, 2011.
3. Gimadiev, R.Sh., *Dinamika myagkikh obolochek parashutnogo tipa* (Dynamics of Parachute-Type Soft Shells), Kazan: Kazan. Gos. Energet. Univ., 2006.
4. Teimurov, F.D., A Computer-Aided Solution of the Problem on the Transverse Impact on a Flexible Connection, *Materialy Vsesoyuznogo simpoziuma po rasprostraneniyu uprugoplasticheskikh voln v sploshnykh sredakh* (Proc. All-Union Symposium on Propagation of Elastoplastic Waves in Continuum), Baku, pp. 182–192, 1966.
5. Gimadiev, R.Sh., Dinmukhametov, F.F., and Galimullin, N.R., Calculation of Spatial Dynamics of Power Transmission Lines under the Joint Action of Wind and Weight Loads, *Izv.Vuz, Problemy Energetiki*, 2010, nos. 3–4, pp. 28–37.
6. Feodos'ev, V.I., *Izbrannye zadachi i voprosy po soprotivleniyu materialov* (Selected Problems on Strength of Materials), Moscow, 1973.
7. Kuhling, H., *Handbook of Physics*, VEB Fachbuchverlag, Leipzig, 1980.